World Academy of Science, Engineering and Technology
International Journal of Aerospace and Mechanical Engineering
Vol:11, No:1, 2017

Investigation on the Bogie Pseudo-Hunting Motion of a Reduced-Scale Model Railway Vehicle Running on Double-Curved Rails

Barenten Suciu, Ryoichi Kinoshita

***Abstract*—**In this paper, an experimental and theoretical study on the bogie pseudo-hunting motion of a reduced-scale model railway vehicle, running on double-curved rails, is presented. Since the actual bogie hunting motion, occurring for real railway vehicles running on straight rails at high travelling speeds, cannot be obtained in laboratory conditions, due to the speed and wavelength limitations, a pseudo-hunting motion was induced by employing double-curved rails. Firstly, the test rig and the experimental procedure are described. Then, a geometrical model of the double-curved rails is presented. Based on such model, the variation of the carriage rotation angle relative to the bogies and the working conditions of the yaw damper are clarified. Vibration spectra recorded during vehicle travelling, on straight and double-curved rails, are presented and interpreted based on a simple vibration model of the railway vehicle. Ride comfort of the vehicle is evaluated according to the ISO 2631 standard, and also by using some particular frequency weightings, which account for the discomfort perceived during the reading and writing activities. Results obtained in this work are useful for the adequate design of the yaw dampers, which are used to attenuate the lateral vibration of the train car bodies.

***Keywords*—**Double-curved rail, octave analysis, lateral vibration, ride comfort, yaw damper, railway vehicle.

I. Introduction

IN order to improve the ride comfort of large train carriages, running at high speeds, amplitude of lateral vibration, which is mainly produced by the bogie hunting motion, should be reduced. Transmitted to the displays of notebook and tablet computers, increasingly used by the railway passengers, such lateral vibration might be the source for blurred images, visual discomfort, headache, dizziness, nausea, and so on. An extensive literature, including standards [1], handbooks [2], and research papers [3], is dedicated to evaluation of the human response at various types of vibration in general, and to estimation of the ride comfort of vehicles in particular, including railway- [4], [5], and auto-vehicles [6]-[8]. Early evaluation methods of the ride comfort were proposed by assuming some specific postures of the human body relative to the vibration direction(s), but the involvement of human subjects in some particular activities was not considered. However, several advanced methods of comfortableness evaluation were proposed under the implicit assumption that the human subjects are involved in some specific activities, such as reading of printed materials [9], and numerical displays [10], as well as writing activities [11].

Since yaw dampers and traction links are the main paths of vibration transmission from bogie to car body, they should be designed to allow for large force transmission at lower frequencies, but to behave as vibration isolators in the domain of relatively higher frequencies, such selective frequency behavior being achieved through the usage of displacement dependent rubber bushes [12], [13], and the employment of colloidal dampers [14].

In this work, the bogie pseudo-hunting motion of a reduced-scale model railway vehicle, running on double-curved rails is theoretically and experimentally investigated. Bogie hunting motion occurs for the real railway vehicles (e.g., bullet trains) during running on straight rails at high travelling speeds (e.g., 200-300 km/h) and long wavelengths (e.g., 20-30 m). Since due to the speed and space limitations, such conditions cannot be duplicated in laboratory, a pseudo-hunting motion was induced by employing convex-concave curvilinear rails. Firstly, the test rig, the system of vibration measurement and ride comfort evaluation, and the experimental procedure are described. Next, a model to clarify the kinematics of the carriage and bogies, as well as, the stroke of the yaw damper, against the particular geometry of the curvilinear rails, is suggested. Resonant peaks observed on the recorded vibration spectra during vehicle travelling, on straight and double-curved rails, are interpreted based on the natural frequencies of various elastic elements used in the construction of the railway vehicle. Ride comfort is evaluated according to the ISO 2631 standard, and also by using the specific filters that account for the discomfort sensation, during the reading and writing activities.

II. Test Rig and Experimental Procedure

Fig. 1 illustrates the main components of the test rig and the measurement equipment used during the running tests of the reduced-scale model railway vehicle.

Railway vehicle consists of two bogies and a carriage frame (Fig. 2), which is connected to bogies via joints (ball bearings) of vertical axis of rotation. Distance between joints is L_1 = 900 mm. Bogies can be driven independently by electrical motors via sprockets and chain transmissions. Maximal driving torque given by motor, at the contact of wheels with rails, is of 1.2 Nm.

Barenten Suciu is with the Department of Intelligent Mechanical Engineering, Fukuoka Institute of Technology, Fukuoka, 811-0295 Japan (phone: +81-92-606-4348; fax: +81-92-606-0747; e-mail: suciu@fit.ac.jp).

Ryoichi Kinoshita is with the Graduate School of Engineering, Fukuoka Institute of Technology, Fukuoka, 811-0295 Japan (e-mail: mcm16104@bene.fit.ac.jp).

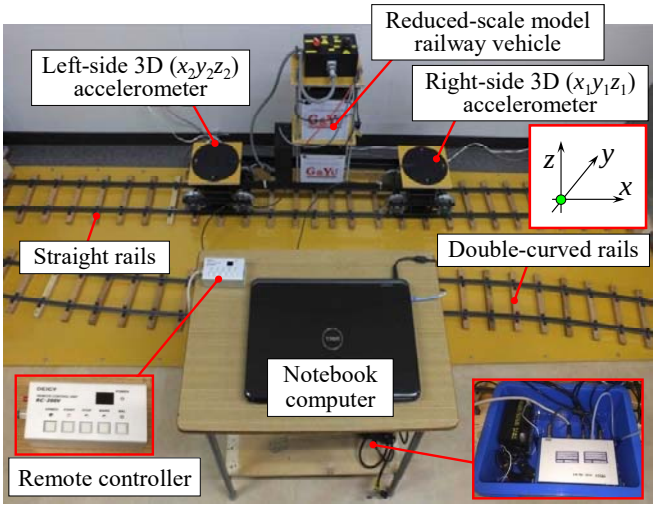

Fig. 1 Photograph of the test rig and the measurement equipment used during the running tests of the reduced-scale model railway vehicle

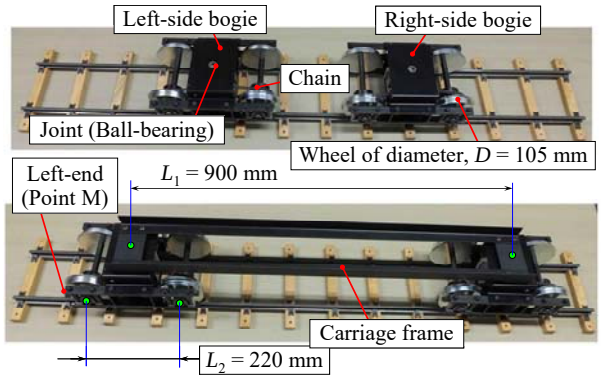

Fig. 2 Constructive details of the reduced-scale model railway vehicle

Two batteries, placed on the carriage frame (see Fig. 1), are used to supply power, via a driving unit, to the bogie motors.

A controller is employed to change the rotation speed of the motor, and hence, to adjust the travelling speed of the vehicle, up to a maximal value of 1 m/s. Motors can be also employed as brakes to stop the bogies.

Each bogie has a mass of M_b = 10 kg, and the carriage frame has a mass of M_c = 25 kg. Railway vehicle is supported by eight wheels (four wheels per bogie). Wheel diameter is D = 105 mm. Distance between wheels of the same bogie is L_2 = 220 mm.

A 3D accelerometer sheet is placed on each bogie, in such a way that center of the accelerometer superposes on the bogie's center. Axes x, y, and z are taken along the longitudinal, lateral, and vertical directions of the bogie, i.e., axes x and y are able to rotate in the horizontal plane as the bogie changes its position on the double-curved rails. On the other hand, rotation of axes does not occur during travelling on straight rails. Signals provided by the right-side and left-side accelerometers are denoted by subscripts 1 and 2, respectively. System of vibration measurement and ride comfort evaluation used in this work is a so-called DEICY system, described in detail elsewhere [8].

Reciprocating travelling tests of the reduced-scale model railway vehicle were performed on relatively short rails (see Fig. 3) at two average speeds V of 0.1 and 0.2 m/s, respectively. Controller was set to stop the vehicle at both ends of the rails, in close proximity of the stopper, just before touching it (Fig. 3).

Since in this work quite detailed information concerning the relatively complex lateral vibration is needed, a third octave analysis of the recorded response is performed, by splitting the interest range of frequency into bands with a bandwidth of one third octave. Usual octave band is a frequency range where the highest limit frequency is twice the lowest limit, and all frequencies below and above these limits are rejected. Further detailed information can be acquired by using a third octave, which has a 1/3 width of that of an octave band, as illustrated by Table I.

Fig. 3 shows the geometry of the double-curved and straight rails. Stoppers are provided at both ends of the rails, to avoid the derailment of the vehicle. Both types of rails have the same total length ($2L$ = 1.5 m × 2 parts = 3 m), average span (B_0 = 136 mm), and pitch of the wood support elements (L_0 = 100 mm).

TABLE I
FREQUENCIES FOR ONE THIRD OCTAVE ANALYSIS

Lower limit frequency [Hz]		Center frequency [Hz]		Upper limit frequency [Hz]	
0.56	28.1	0.63	31.5	0.71	35.4
0.71	35.6	0.8	40	0.90	44.9
0.89	44.5	1	50	1.12	56.1
1.11	56.1	1.25	63	1.40	70.7
1.43	71.3	1.6	80	1.80	89.8
1.78	89.1	2	100	2.25	112.3
2.23	111.4	2.5	125	2.81	140.3
2.81	142.5	3.15	160	3.54	179.6
3.56	178.2	4	200	4.49	224.5
4.45	222.7	5	250	5.61	280.6
5.61	280.6	6.3	315	7.07	353.6
7.13	356.3	8	400	8.98	449.0
8.9	445.4	10	500	11.2	561.3
11.1	561.2	12.5	630	14.0	707.2
14.3	712.7	16	800	18.0	898.0
17.8	890.9	20	1000	22.5	1122.5
22.3	1113.6	25	1250	28.1	1403.1

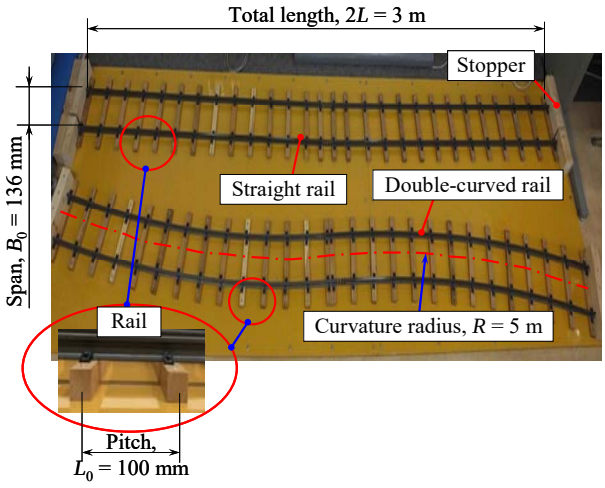

Fig. 3 Photograph of the employed straight and double-curved rails

Double-curved rail consists of two circular arcs, each having a mean curvature radius of R = 5 m. These arcs are joined together to produce a convex-concave curvilinear rail.

III. Geometrical Model of the Double-Curved Rails

By neglecting the influence of the span B_0 (see Fig. 3) on the rails geometry, Fig. 4 presents a simplified geometrical model of the middle double-curved line. Such model is necessary to link the experimental results with the geometry of the railway vehicle, and also with the specific geometry of the rails. Thus, Fig. 5 presents the relationship between the rotation angle Γ of the carriage frame and the system of coordinates attached to the bogie joints 1 and 2, i.e., to the accelerometers shown in Fig. 1.

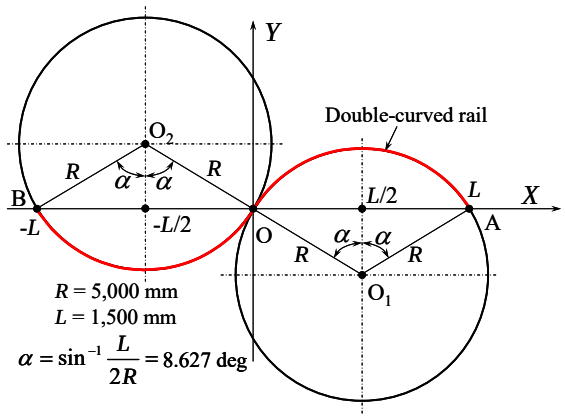

Fig. 4 Simplified geometrical model of the double-curved rails

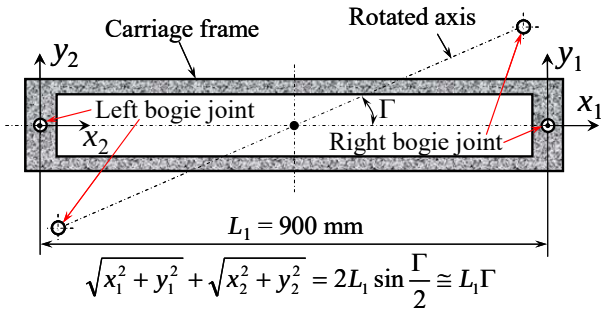

Fig. 5 Relationship between the rotation angle of the carriage frame and the system of coordinates attached to the left and right bogie joints

Based on such geometrical model, the angle of rotation Γ can be calculated as:

$$\Gamma = \begin{cases} \theta_M + \beta & for \\ -L + \dfrac{D}{2}\cos(\alpha-\gamma) \le X_M \le -L_1\cos(\alpha-\beta) & \\ \cos^{-1}\left[\dfrac{2\sin\alpha - \sin\theta_N - \sin\theta_M}{2\sin\beta}\right] & for \\ -L_1\cos(\alpha-\beta) \le X_M \le 0 & \\ \theta_M - \beta & for \\ 0 \le X_M \le L - \dfrac{D}{2}\cos(\alpha-\gamma) - L_1\cos(\alpha-2\gamma-\beta) & \end{cases} \quad (1)$$

where X_M is the coordinate of the point M shown on Fig. 2, i.e., the left-end of the railway vehicle. The various angular parameters used in (1) are given by the following expressions.

Angle θ_M

$$\theta_M = \begin{cases} \sin^{-1}\dfrac{0.5L + X_M}{R} & ; \quad -L \le X_M \le 0 \\ \sin^{-1}\dfrac{0.5L - X_M}{R} & ; \quad 0 \le X_M \le L \end{cases} \quad (2)$$

Angle θ_N

$$\theta_N = \tan^{-1}\frac{\sin\theta_M - 2\sin\alpha}{\cos\theta_M - 2\cos\alpha} - \cos^{-1}\frac{2\cos^2\beta + 1 - 2\cos(\theta_M - \alpha)}{\sqrt{5 - 4\cos(\theta_M - \alpha)}} \quad (3)$$

Angle α

$$\alpha = \sin^{-1}\frac{L}{2R} = \sin^{-1}(0.15) = 8.627 \text{ deg} \quad (4)$$

Angle β

$$\beta = \sin^{-1}\frac{L_1}{2R} = \sin^{-1}(0.09) = 5.164 \text{ deg} \quad (5)$$

Angle γ

$$\gamma = \sin^{-1}\frac{D}{4R} = \sin^{-1}(0.00525) = 0.301 \text{ deg} \quad (6)$$

Next, Fig. 6 illustrates the variation of the rotation angle Γ of the carriage frame versus the coordinate X_M of the left-end point M of the railway vehicle, as calculated by using (1)-(6).

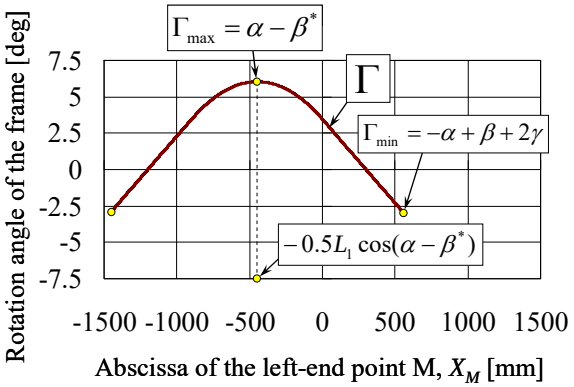

Fig. 6 Variation of the rotation angle of the carriage frame versus the abscissa of the left-end point M of the railway vehicle, during travelling on the double-curved rails

A symmetrical mountain-like graph is obtained relative to the vertical line passing through $X_M = -0.5L_1\cos(\alpha - \beta^*) = -447.5$ mm, where the corresponding angle β^* is given by:

$$\beta^* = \sin^{-1}\frac{L_1}{4R} = \sin^{-1}(0.045) = 2.579 \text{ deg} \quad (7)$$

Thus, maximal Γ_{max} and minimal Γ_{min} values of the carriage frame rotation angles are obtained, as:

$$\Gamma_{max} = \alpha - \beta^* = 6.048 \text{ deg}, \quad (8)$$

and

$$\Gamma_{min} = -\alpha + \beta + 2\gamma = -2.861 \text{ deg}, \quad (9)$$

respectively (see Fig. 6).

IV. Working Conditions of the Yaw Damper

Yaw dampers are absorbers laterally connected between the bogie and car body, but parallel to the railways direction. The main purpose of such absorbers is to attenuate the vibration produced by the left-right lateral irregularities of the railways, as well as by the lateral winds. Thus, they are used to suppress the bogie hunting motion, and to improve travelling stability of the real railway vehicle [14].

Although in this work yaw dampers are not placed on the reduced-scale railway vehicle, based on the geometrical model described in the previous section, the working conditions of the yaw dampers can be clarified, for such particular geometry of the rails. In other words, results obtained in this work are useful for the adequate design of yaw dampers, which, in our future work, will be attached to the reduced-scale railway vehicle. Thus, Fig. 7 presents the length of the yaw damper for nil rotation angle Γ of the carriage frame relative to the bogie. On the other hand, Fig. 8 (a) shows the minimal length, and Fig. 8 (b) illustrates the maximal length of the yaw damper obtained for the extreme values of the rotation angle, i.e., $\pm\beta$.

According to the geometry illustrated in Fig. 8, the maximal and minimal length of the yaw damper can be calculated as:

$$\begin{cases} a_{max} = \sqrt{(a_0 + b\sin\beta)^2 + (2b\sin^2\frac{\beta}{2})^2} \\ a_{min} = \sqrt{(a_0 - b\sin\beta)^2 + (2b\sin^2\frac{\beta}{2})^2} \end{cases} \quad (10)$$

Under the reasonable assumption that the mean length of the yaw damper approximately equals its length at nil rotation angle of the carriage frame:

$$a_{mean} = \frac{a_{max} + a_{min}}{2} \cong a_0 \quad (11)$$

one obtains the following, approximate but quite precise relationship for the stroke S of the yaw damper:

$$S = a_{max} - a_{min} \cong 2b\sin\beta = b\frac{L_1}{R} \quad (12)$$

In conclusion, (12) implies that the stroke of the yaw damper varies directly proportionally to the distance L_1 between the bogie joints, and to the eccentricity b of the yaw damper axis relative to the bogies joint axis. On the other hand, the stroke depends inversely proportionally on the curvature radius R of the rails. This result agrees with the well-known fact that nil stroke of the yaw damper is achieved during travelling of the railway vehicle on straight rails ($R \to \infty$).

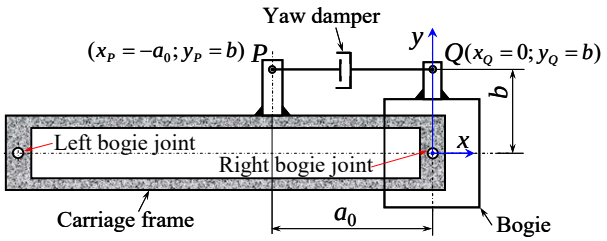

Fig. 7 Length of the yaw damper for nil rotation angle of the carriage frame relative to the bogie

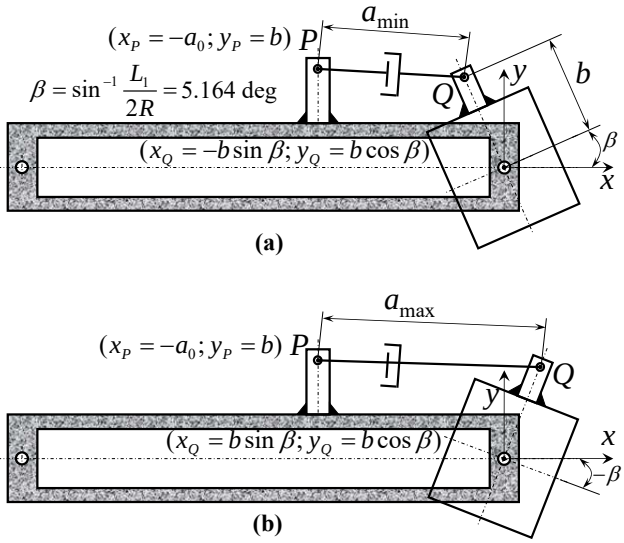

Fig. 8 (a) Minimal length, and (b) maximal length of the yaw damper obtained for the extreme values of the rotation angle

V. Experimental Results

Fig. 9 presents the variation of the longitudinal a_{x1}, lateral a_{y1}, and vertical a_{z1} accelerations versus frequency, recorded at the right joint of the carriage frame (see Fig. 5), for a speed $V = 0.2$ m/s of the railway vehicle travelling on the double-curved rails.

As desired, the lateral acceleration displays the highest peak, which corresponds to a pseudo-hunting motion of the scale model railway vehicle. In the other words, since the actual bogie hunting motion, occurring for real railway vehicles running on straight rails at high travelling speeds, cannot be obtained in laboratory conditions due to the speed and wavelength limitations, a pseudo-hunting motion was successfully induced here by using the double-curved rails of particular geometry. Hence, ride comfort of the vehicle will be mainly determined by the frequency characteristics of the lateral acceleration. For this reason, the following analysis focuses on the lateral movement of the railway vehicle. Thus, Fig. 10 shows the variation of the lateral acceleration a_{y2}, measured at the left joint of the carriage frame, versus frequency for two travelling speeds ($V = 0.1$ and 0.2 m/s) of the

railway vehicle running on straight and double-curved rails. Note that the highest resonant peak of the lateral acceleration increases at augmentation of the travelling speed. On the other hand, by reducing the curvature radius of rails from infinity for the straight rails, to R = 5 m for the double-curved rails, the resonant peak is considerably augmented.

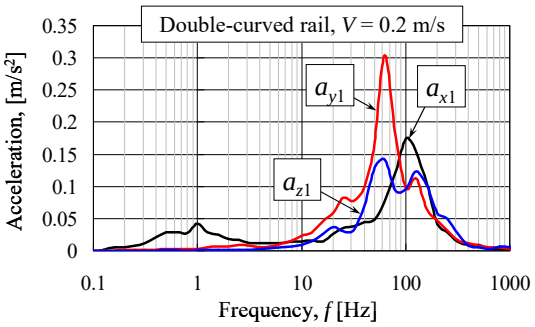

Fig. 9 Variation of the axial, lateral and vertical accelerations versus frequency, recorded at the right joint of the carriage when the railway vehicle travelled on the double-curved rails at a speed of 0.2 m/s

For comparison, Fig. 11 illustrates the variation of the lateral acceleration a_{y1}, determined at the right joint of the carriage frame, versus frequency when the railway vehicle travels at a speed V = 0.2 m/s on straight and double-curved rails. Note that quite similar vibration spectra were recorded at both the right and left joints of the carriage frame, due to the structural and geometrical symmetry of the investigated system. Regardless the shape of the rails, mainly three resonant peaks (see Fig. 11) can be distinguished. They are denoted as 1st, 2nd, and 3rd peak, and correspond to the following frequencies: f_1 = 25 Hz, f_2 = 63 Hz and f_3 = 125 Hz, respectively. These frequencies are related to the natural frequencies of various elastic elements (see Figs. 12 and 13), and can be simply calculated as follows.

1st peak is related to natural frequency of the helical spring:

$$f_1 = \frac{1}{2\pi}\sqrt{\frac{16K_S}{M_c}} \tag{13}$$

where M_c = 25 kg is the mass of the carriage frame and K_S = 38.6 N/mm is the stiffness of the helical compression spring (16 helical springs per vehicle, see Figs. 12 and 13).

2nd resonant peak is related to the natural frequency produced by the rotational mode of vibration of the carriage frame:

$$f_2 = \frac{1}{2\pi}\sqrt{\frac{K_R}{J}} \tag{14}$$

where J = 560 kg·mm² is the moment of inertia, and K_R = 88 N·m/rad is the rotational stiffness of the carriage frame along the longitudinal axis of the railway vehicle (see Fig. 13).

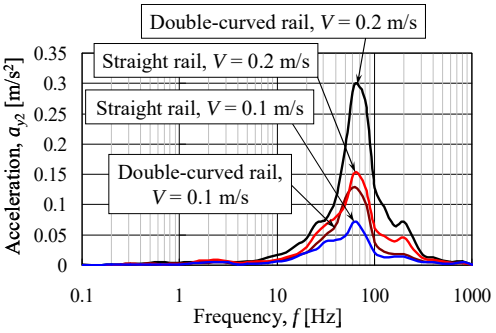

Fig. 10 Variation of the lateral acceleration, measured at the left joint of the carriage frame, versus frequency for two travelling speeds of the railway vehicle running on straight and double-curved rails

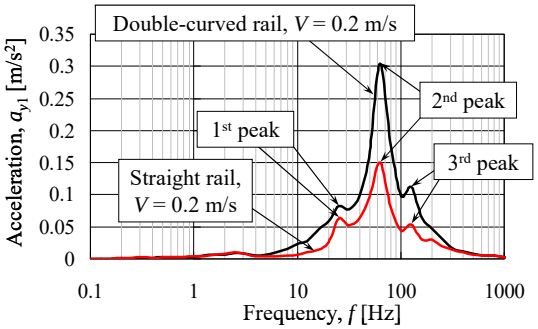

Fig. 11 Variation of the lateral acceleration, measured at the right joint of the carriage frame, versus frequency when the railway vehicles travel at a speed of 0.2 m/s on straight and double-curved rails

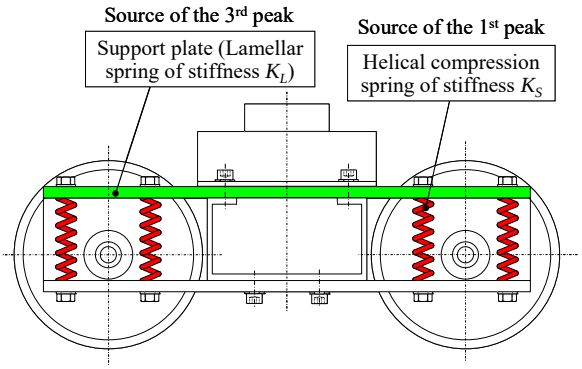

Fig. 12 Schematic frontal view of the railway vehicle, the carriage frame being supported by 16 helical compression springs (8 springs per bogie) and 8 lamellar springs (4 springs per bogie)

3rd resonant peak corresponds to the natural frequency of the lamellar spring:

$$f_3 = \frac{1}{2\pi}\sqrt{\frac{8K_L}{M_c}} \tag{15}$$

where K_L = 1,928 N/mm is the stiffness of the lamellar spring (8 lamellar springs per vehicle, see Figs. 12 and 13).

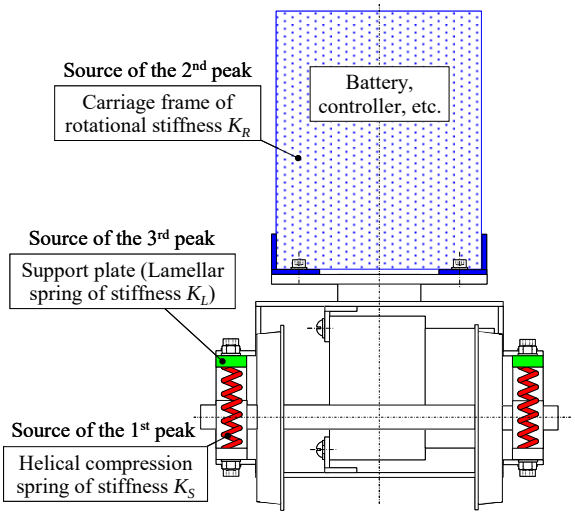

Fig. 13 Schematic lateral view of the railway vehicle, the carriage frame being able to rotate along the longitudinal axis of the vehicle

VI. Ride Comfort Evaluation

Fig. 14 illustrates the variation of the frequency weighting G used by the K factor method for ride comfort evaluation [6]:

$$G(f_i)=\begin{cases}10^{(3f_i-15)/20} & ,\ 0\le f_i\le 4\\ 10^{-3/20} & ,\ 4\le f_i\le 8\\ 10^{(-0.75f_i+3)/20} & ,\ f_i\ge 8\end{cases} \tag{16}$$

and the frequency weightings W_c, W_d, W_k used by the ISO 2631 standard [1] for ride comfort evaluation are

$$\begin{cases} W_c(f_i)=5.04\cdot\Delta(f_i)\cdot\Omega_c(f_i)\\ W_d(f_i)=1.26\cdot\Delta(f_i)\cdot\Omega_d(f_i)\\ W_k(f_i)=7.875\cdot\Delta(f_i)\cdot\Omega_k(f_i)\cdot\Psi(f_i)\end{cases} \tag{17}$$

where the function $\Delta(f_i)$ is given by:

$$\Delta(f_i)=\frac{f_i^2}{\sqrt{0.0256+f_i^4}}\frac{10^4}{\sqrt{10^8+f_i^4}} \tag{18}$$

and where the functions $\Omega_c, \Omega_d, \Omega_k(f_i)$ are given by:

$$\begin{cases}\Omega_c(f_i)=\sqrt{\dfrac{f_i^2+64}{0.3969f_i^4+13.1968f_i^2+1625.7024}}\\ \Omega_d(f_i)=\sqrt{\dfrac{f_i^2+4}{0.3969f_i^4+0.8248f_i^2+6.3504}}\\ \Omega_k(f_i)=\sqrt{\dfrac{f_i^2+156.25}{0.3969f_i^4+32.2188f_i^2+9689.9414}}\end{cases} \tag{19}$$

and also where the function $\Psi(f_i)$ is given by:

$$\Psi(f_i)=\sqrt{\frac{0.8281f_i^4-3.6858f_i^2+26.1262}{0.8281f_i^4-7.3642f_i^2+104.2947}} \tag{20}$$

versus the excitation frequency f_i. It is useful to note that these particular excitation frequencies f_i, recommended by various standards and methods proposed for the evaluation of the ride comfort, are the same with the center frequencies employed by the third octave analysis (see Table I).

Frequency band of the filter G is 0.1-100 Hz (Fig. 14), and its maximal gain of 0.708 occurs in the frequency range of 4-8 Hz. Since such filter can be used only for vertical vibrations, it cannot be employed for estimation of the ride comfort of the railway vehicle subjected to lateral excitation. On the other hand, the frequency band of the filters proposed by the ISO standard (W_c, W_d, W_k) is of 0.1-400 Hz (Fig. 14). Their maximal gains are of 1.024, 1.013, and 1.054, occurring at frequencies of 3.7 Hz, 1.1 Hz, and 6.2 Hz, respectively.

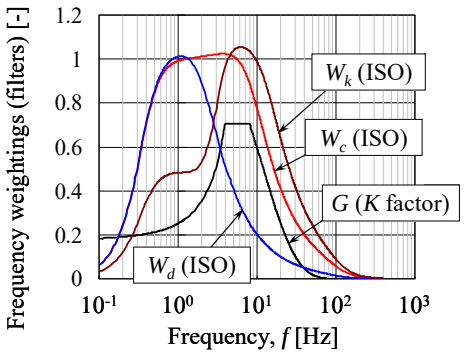

Fig. 14 Variation of the frequency weightings (filters), used by the K factor method, and by the ISO 2631 standard for ride comfort evaluation, versus the excitation frequency

Filtering process of the acceleration signal is depending on the specific location of the accelerometers used, i.e., feet, seat and seat-back surfaces, as well as on the specific axis of the 3D Cartesian system of coordinates [1]. Concretely, an equivalent, i.e., a weighted and composite acceleration a_w is calculated as [8]:

$$a_w=\sqrt{\sum_i a_i^2} \tag{21}$$

where

$$a_i^2=[W_c^2\frac{16a_{xB}^2}{25}+W_d^2(\frac{a_{yB}^2}{4}+\frac{4a_{zB}^2}{25}+a_{xS}^2+a_{yS}^2)+ \\ +W_k^2(a_{zS}^2+\frac{a_{xF}^2+a_{yF}^2}{16}+\frac{4a_{zF}^2}{25})]_i \tag{22}$$

In (22), a represents the acceleration along the axes of a 3D Cartesian system of coordinates (subscripts x, y and z) measured at the feet surface (subscript F), at the seat surface

(subscript *S*) and at the seat-back surface (subscript *B*), respectively. Then, the human perception of the vibration level is evaluated as follows [1], [8]:

for $a_w < 0.315$ m/s^2, "comfortable";
for 0.315 m/s$^2 \le a_w \le$ 0.63 m/s^2, "a little uncomfortable";
for 0.5 m/s$^2 \le a_w \le$ 1.0 m/s^2, "fairly uncomfortable";
for 0.8 m/s$^2 \le a_w \le$ 1.6 m/s^2, "uncomfortable";
for 1.25 m/s$^2 \le a_w \le$ 2.5 m/s^2, "very uncomfortable"; and
for $a_w \ge 2.0$ m/s^2, "extremely uncomfortable".

Considering only the effect of the lateral acceleration for the ride comfort evaluation, (22) reduces to:

$$a_i^2 = [W_d^2 (\frac{a_{yB}^2}{4} + a_{yS}^2) + W_k^2 \frac{a_{yF}^2}{16}]_i \quad (23)$$

Then, under the assumption that the acceleration measured at the feet, seat and seat-back surfaces is the same:

$$a_{yB} = a_{yS} = a_{yF} = a_y \quad (24)$$

the equivalent acceleration (22) reduces to the following form, which is suitable for the ride comfort evaluation of the reduced-scale model railway vehicle studied in this work:

$$a_W = \sqrt{[a_y^2 (\frac{5W_d^2}{4} + \frac{W_k^2}{16})]_i} \quad (25)$$

Based on (25), it becomes possible to define a new frequency weighting (filter) suitable for the evaluation of the ride comfort due to the solely effect of the lateral acceleration, as follows:

$$W_l = \frac{1}{2}\sqrt{5W_d^2 + \frac{W_k^2}{4}} \quad (26)$$

Thus, Fig. 15 illustrates the variation of the filter W_l against the excitation frequency. This filter is compared (see Fig. 15) with other filters previously reported in the literature, such as, the filter proposed solely for the lateral acceleration by [7], and the filters proposed by [11] to take into account for the difficulties to read and write under the lateral vibration exposure. Compared with the filter (26), on one hand, the filter proposed by [7] displays higher values for frequencies lower than about 5 Hz; on the other hand, filters proposed by [11] to take into account the influence of the lateral vibration on the reading and writing activities, exhibits higher values in the range of 2.5-6.3 Hz (Fig. 15). For these reasons, some revisions of the filters to be used for lateral vibration exposure might be necessary, but such subject is not to be addressed by the present work. In these circumstances, filter (26) will be preferred here for the evaluation of the ride comfort of the railway vehicle.

In the end, Table II shows the ride comfort, as estimated by using (25), of the reduced-scale model railway vehicle running on straight and double-curved rails at two values of the travelling speed (V = 0.1 and 0.2 m/s), when the accelerometers are placed at the bogie joints 1, and 2.

As, expected, the equivalent acceleration a_W increases at augmentation of the travelling speed, and at reduction of the curvature radius of the rails from infinity for straight rails, to a finite value for double-curved rails. Similar results are obtained at both locations 1, and 2 of the 3D accelerometers. Since the equivalent acceleration does not exceed the value of 0.315 m/s^2, it appears that the reduced-scale model railway vehicle can be qualified as comfortable.

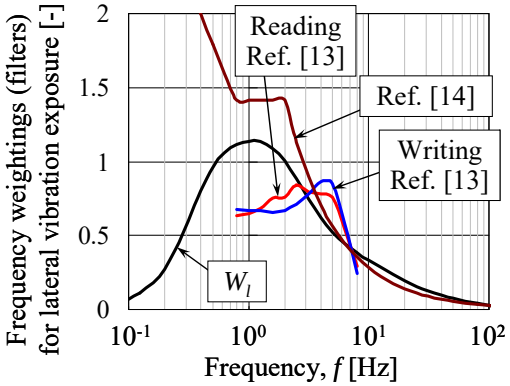

Fig. 15 Variation of the frequency weightings (filters) for ride comfort evaluation under lateral vibration exposure versus the excitation frequency, as proposed in this work and by [7], [11]

TABLE II
RIDE COMFORT EVALUATION OF THE RAILWAY VEHICLE

a_W [m/s^2]	Speed, V = 0.1 m/s		Speed, V = 0.2 m/s	
	Bogie joint 1	Bogie joint 2	Bogie joint 1	Bogie joint 2
Straight rails	0.015	0.015	0.026	0.027
Double-curved rails	0.021	0.020	0.040	0.038

VII. CONCLUSIONS

By employing double-curved rails, a pseudo-hunting motion of a reduced-scale model railway vehicle was successfully achieved. From the experimental and theoretical analysis of the proposed system, the following conclusions can be drawn:

1) When the railway vehicle traveled on double-curved rails, a symmetrical mountain-like graph for the variation of the carriage rotation angle relative to the bogies was obtained, and the extreme values of the carriage rotation angle were clarified.
2) Although in this work yaw dampers are not placed on the reduced-scale model railway vehicle, the working conditions of the yaw dampers were revealed, for the particular geometry of the rails, carriage frame, and bogies.
3) Stroke of the yaw damper varied directly proportionally to the distance between the bogie joints, and to the eccentricity of the yaw damper axis relative to the bogies joint axis. On the other hand, the stroke depended inversely proportionally on the curvature radius of the rails. This agrees with the fact that nil stroke of the yaw damper is

achieved during travelling of the railway vehicle on straight rails, of infinite curvature radius.

4) Resonant frequencies observed on the lateral vibration spectra were found to be related to the natural frequencies of various elastic elements used in the construction of the railway vehicle, such as: helical compression springs, lamellar bending springs, and rotational mode of vibration of the carriage frame.
5) Ride comfort of the vehicle was mainly determined by the lateral acceleration. Resonant peaks of the lateral acceleration increased at augmentation of the travelling speed. Further, by reducing the curvature radius of rails from infinity for straight rails, to a finite value for double-curved rails, the resonant peak was considerably augmented.
6) Particular excitation frequencies recommended by various standards and methods proposed for the evaluation of the ride comfort, are the same with the center frequencies employed by the third octave analysis.
7) A frequency weighting (filter) suitable for the evaluation of the ride comfort due to the exclusive effect of the lateral acceleration was proposed, and compared with other filters previously reported in the literature. Revisions of the filters to be used for lateral vibration exposure might be necessary, but such subject was not decisively addressed by the present work.
8) Results obtained in this work are useful for the adequate design of yaw dampers, which, in our future work, will be attached to the reduced-scale model railway vehicle.

ACKNOWLEDGMENT

This research is mainly supported by the Japanese Ministry of Education, Grant-in-aid for scientific fundamental research, Project C-16K06059. Additional research funds were received from the Electronics Research Institute, affiliated to Fukuoka Institute of Technology, Japan.

The reduced-scale railway vehicle was manufactured by the MITACHI OMOSHIRO Mechanical Workshop from the MITACHI Applied Chemistry Ltd. Authors would like to acknowledge the support of Mr. Noriyuki Okamoto @ SENRO Trading Company for purchasing the rails and railway vehicle.

REFERENCES

[1] ISO 2631 Standard, *Mechanical Vibration and Shock – Evaluation of Human Exposure to Whole-Body Vibration*, 1997, pp. 1–27.
[2] M. J. Griffin, *Handbook of Human Vibration*. London: Academic Press, 2003, 2nd ed., ch. 2–12, pp. 27–530.
[3] O. Thuong, and M. J. Griffin, "The Vibration Discomfort of Standing Persons: 0.5 to 16 Hz Fore – and – Aft, Lateral, and Vertical Vibration," *Journal of Sound and Vibration*, 330(4), pp. 816–826, 2011.
[4] ENV 12299, *Railway Applications – Ride Comfort for Passengers*, 2010.
[5] G. Gallais, H. Ohno, and C. Talotte, "Frequency Weightings for the Evaluation of Discomfort of Standing Passengers on Trains," *Proc. of 9th World Congress on Railway Research*, pp. 1–12, 2011.
[6] S. Komamura, R. Watanabe, K. Mizumukai, T. Mizobuchi, Y. Morita, T. Masamura, J. Arai, H. Matsumoto, W. Tsuji, H. Matsuda, A. Kani, Y. Ono, F. Tsuji, and N. Yoshida, *Automotive Suspension*. Tokyo: Kayaba Technical Publisher, 2005, 2nd ed., pp. 26–68 (in Japanese).
[7] K. Tanifuji, "The Development of Car Vibration Analyzing System for Maintenance of Riding Quality. 1st Report: Outline of the Vibration Analyzing System," *Trans JSME C*, 52(481), pp. 2405–2408, 1986 (in Japanese).
[8] C. V. Suciu, and T. Tobiishi, "Comfortableness Evaluation of an Automobile Equipped with Colloidal Suspensions," *JSME Journal of System Design and Dynamics*, 6(5), pp. 555–567, 2012.
[9] V. Kumar, and V. H. Saran, "A Review of the Performances of Reading Activity by Seated Subjects Exposed to Whole Body Vibration," *International Journal of Mechanical Engineering and Robotics Research*, 1(1), pp. 193–198, 2014.
[10] C. H. Lewis, and M. J. Griffin, "Prediction the Effects of Vertical Vibration Frequency, Combinations of Frequencies and Viewing Distance on the Reading of Numeric Displays," *Journal of Sound and Vibration*, 70(3), pp. 355–377, 1980.
[11] J. Sundstrom, *Difficulties to Read and Write Under Lateral Vibration Exposure*. Stockholm: Doctoral Thesis, Royal Institute of Technology Aeronautical and Vehicle Engineering, Rail Vehicles, 2007, pp. 56–58.
[12] T. Tomioka, T. Takigami, A. Fukuyama, and T. Suzuki, "Prevention of Carbody Vibration of Railway Vehicles Induced by Imbalanced Wheelsets with Displacement Dependent Rubber Bush," *Journal of Mechanical Systems for Transportation and Logistics*, 3, pp. 131–142, 2010.
[13] T. Tomioka, and T. Takigami, "Reduction of Bending Vibration in Railway Vehicle Carbodies using Carbody-Bogie Dynamic Interaction," *Vehicle System Dynamics*, 48, pp. 467–486, 2010.
[14] B. Suciu, and T. Tomioka, "Experimental Investigation on the Elastic and Dissipative Characteristics of a Yaw Colloidal Damper Destined to Carbody Suspension of a Bullet Train," *Journal of Physics: Conference Series*, 744(012142), pp. 1–11, 2016.

Barenten Suciu was born on July 9, 1967. He received Dr. Eng. Degrees in the field of Mech. Eng. from the Polytechnic University of Bucharest, in 1997, and from the Kobe University, in 2003. He is working as Professor at the Department of Intelligent Mech. Eng., Fukuoka Institute of Technology. He is also entrusted with the function of Director of the Electronics Research Institute, affiliated to the Fukuoka Institute of Technology. He is member of JSME and JSAE. His major field of study is the tribological and dynamical design of various machine elements.

Ryoichi Kinoshita was born on December 29, 1993. He received the Eng. Degree from Fukuoka Institute of Technology, in 2015. He is a master-course student at the Graduate School of Engineering, Fukuoka Institute of Technology. His research interests are in the field of vibration absorbers for railway vehicles.